Can we image guided waves by elastic full waveform inversion?

Biondo Biondi, Ariel Lellouch, Ettore Biondi and Stuart Farris

ABSTRACT

We investigate the feasibility, and potential advantages, of applying elastic full-waveform inversion to guided waves generated by perforation shots and recorded by a distributed acoustic sensing fiber cemented into a horizontal well. Since a correct source model is essential for waveform inversion, we first show that the amplitudes and phases observed in the field data are better modeled using a dipole source than a monopole source. We then illustrate the high-resolution potential of waveform inversion by comparing data modeled assuming a horizontally layered medium with and without a thin high-velocity layer in the reservoir. Significant phase differences are observed with a two-meter thick high-velocity layer, and smaller, but still visible, phase differences are observed with a one-meter thick intrusion. Finally we analyze the data residuals of a first iteration of a hypothetical waveform inversion process when the starting model is a vertical average of the true model. We show that data-residuals phases at either short offsets ($\leq$150 m), or at low frequencies ($\leq$80 Hz), are sufficiently close to the corresponding phases of data modeled with the starting model. This result indicate that a waveform inversion process carefully bootstrapped from near offsets and low frequencies should not suffer from cycle skipping.

INTRODUCTION

In Lellouch et al. (2019b) and Lellouch et al. (2019a) we have reported the observation and modeling of DAS recordings of guided waves generated by perforation shots fired in the same well as the fiber, as well as by perforation shots fired in a nearby lateral (Lellouch et al., 2019c). These high-frequency densely sampled data may lead to imaging of unconventional reservoirs with unprecedented resolution, and possibly enable the imaging of reservoir-properties changes related to stimulation and production.

Thanks to the high receiver density of DAS recording systems, the recorded data represent an unaliased subset of the propagating wavefields and thus should support imaging by full waveform inversion (FWI). Furthermore, since we are observing both P-waves and S-waves arrivals, and elastic phenomena are likely to play an important role in accurately modeling both phases ad amplitudes of the guided waves, we should consider performing elastic FWI (EFWI) on this new kind of data.

In this report we explore the feasibility of EFWI performed on DAS recording of the observed guided waves. We focus on the utilization of data recorded by fibers in the same well that is being perforated and stimulated because we have only a 2D elastic modeling program available. Modeling and inversion in 3D would be computationally expensive, but within the reach of high-performance computational systems available to us. However, some of our considerations are also valid for the interesting case of data recorded by fibers in a well parallel to the well that is being perforated and stimulated. We first discuss what is an appropriate source model for the perforation shots. We then explore by an example the resolution limits of EFWI geared for imaging thin layers in the reservoir. Finally, we discuss potential convergence problems of an EFWI process caused by cycle-skipping.

MODELING PERFORATION SHOTS AS ELASTIC SOURCES

Full waveform inversion is sensitive to amplitudes as well as the phases of the recorded wavefield. In particular, elastic waveform inversion is also sensitive to relative amplitudes between P and S waves. The relative amplitudes observed in field data recorded by a fiber in the same borehole where perforation shots were fired (i.e. single-well acquisition) are not well modeled by the simple elastic modeling shown by Lellouch et al. (2019a). Field data show strong P arrivals and weak S arrivals; in contrast, the modeled elastic data show stronger S arrivals than P arrivals. The most likely reason for this discrepancy is that we modeled the perforation as a simple monopole source (vertical force), whereas a dipole is a better model for a perforation in a fluid-filled borehole (Fehler and Pearson, 1984). In this section, we compare data modeled using a monopole source with data modeled using a dipole source for single-well recording. We also show a theoretical modeling of the recorded amplitudes when the perforation shots are fired in a horizontal well parallel to the recording well (cross-well acquisition). These results are relevant to the analysis of the field data shown in Lellouch et al. (2019c).

Monopole vs. dipole radiation patterns

We compare two different source mechanisms. The first is a directional source applied in the depth direction perpendicular to the well. It is introduced as particle velocity in that direction, acting as a monopole source. However, Fehler and Pearson (1984) show that for a fluid-filled borehole, which is the case in the field acquisiton, the source mechanism is better approximated as a dipole. They approximate the perforation shot as a local increase in borehole diameter. The source function is then of the form of the following diagonal stress tensor,

$$M = A \begin{pmatrix} \lambda + \mu & 0 \\ 0 & \lambda \end{pmatrix}, \tag{1}$$

where λ, μ are the Lamé parameters, A is a constant and the first row corresponds to the horizontal component and the second one to the vertical component. In Figure 1 we illustrate the radiation patterns of the two sources by showing the snapshots of the amplitude of the particle velocity vector generated by the sources injected in a homogeneous elastic medium. For a monopole source (panel a), the P-waves are weak along the horizontal direction while S-waves are stronger. However, for a dipole source (panel b) P-waves dominate. While the behavior for guided waves is slightly different, we deduce that the basic source mechanism for perforation shots generates weak S guided waves along the well, which is consistent with field data observations. Fehler and Pearson (1984) derive the following analytic approximation of the far-field amplitudes for P and S waves, respectively:

$$\begin{aligned} A_P &\propto 1/V_P^2 \cdot 1/R \cdot \left[\lambda + \mu - \mu \cdot cos^2(\phi)\right] \\ A_S &\propto 1/V_S^2 \cdot 1/R \cdot \left[(\lambda + \mu) \cdot |sin(2\phi)|\right], \end{aligned} \tag{2}$$

which is consistent with the snapshots shown in Figure 1.

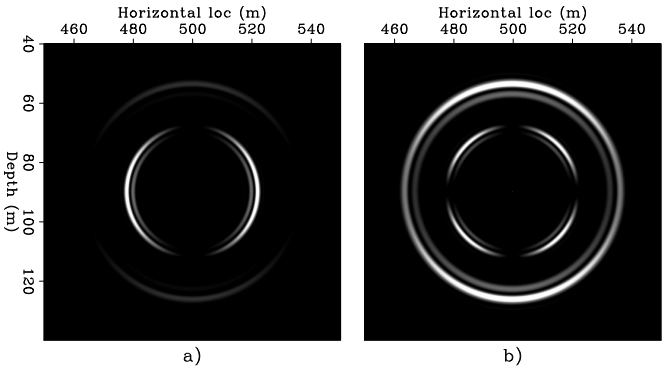

Figure 1: Snapshots of wavefield amplitudes for sources injected in a homogeneous elastic medium: a) monopole, and b) dipole. [**NR**]

Guided-waves modeling

Radiation patterns such as the ones illustrated in Figure 1 are useful for determining amplitudes of body waves propagating in a homogeneous, or smoothly varying, medium. As we are interested in modeling and imaging guided waves, we repeat the comparison between monopole and dipole sources for a more realistic horizontally-layered model. Figure 2 shows the elastic parameters: P-waves velocity (V_P), S-waves velocity (V_S), and density as a function of depth. We compare the particle velocity along the direction of the well computed assuming this model and injecting both sources. The data recorded at the same depth (100 meters) as the sources are shown in Figure 3. A monopole source (panel a) excites both P- and S- guided waves. This shows that the shale formation can act as a waveguide for both types of waves. In contrast, for the dipole source (panel b) the guided P waves are much stronger than the guided S-waves; a behavior similar to the one we observe in the field data. Furthermore, as the dipole source generates P energy propagating exactly in the horizontal direction, the P guided-waves arrivals are more continuous, albeit with rotating phase

as a function of offsets, for a dipole source than for a monopole source. This data characteristic is also consistent with the field data shown in Lellouch et al. (2019b).

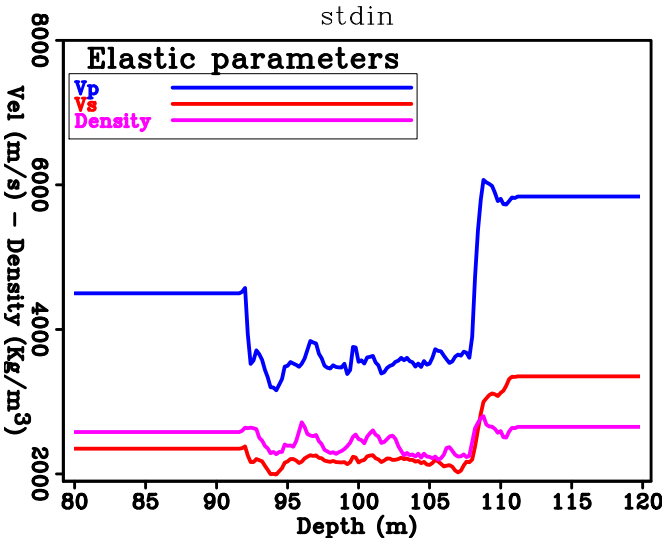

Figure 2: Elastic parameters for a realistic 1-D model. Subsurface properties vary with depth only. The shale formation has low V_P,V_S and density. Source and receivers were placed at a depth of 100 m [**NR**]

Radiation pattern for a cross-well acquisition

The dipole nature of the perforation shot is important for cross-well acquisition. For such a case, the fact that DAS systems measure strain along the direction of the fiber induces an angle-dependent behavior, as can be followed in Martin (2018). The combination of the source radiation and the strain measurement along the direction of the recording DAS yields the following behavior for P (A_P) and S (A_S) waves after correction for geometrical spreading:

$$\begin{aligned} A_P &\propto \frac{1}{\lambda+\mu} \cdot cos^2(\phi) \cdot \left[\lambda + \mu - \mu \cdot cos^2(\phi)\right] \\ A_S &\propto \frac{\lambda+\mu}{\mu} \cdot sin(2\phi) \cdot |sin(2\phi)|, \end{aligned} \tag{3}$$

For a distance of 260 m between wells and representative Lamé parameters, the P- and S- relative amplitudes are shown in 4. They are plotted as a function of horizontal distance between source and receiver. For a distance of zero, the receiver is directly in front of the source. In this case, both P- and S- waves fade. At increasing horizontal distances, the S-waves amplitude grows until an angle of 45 degrees (horizontal distance equal to distance between the wells), and then decrease. The P-waves amplitude is increasing with horizontal distance. Notice that these amplitudes plots do not take into account attenuation that is present in field data, where we observe a decay in P-waves amplitudes at large offsets.

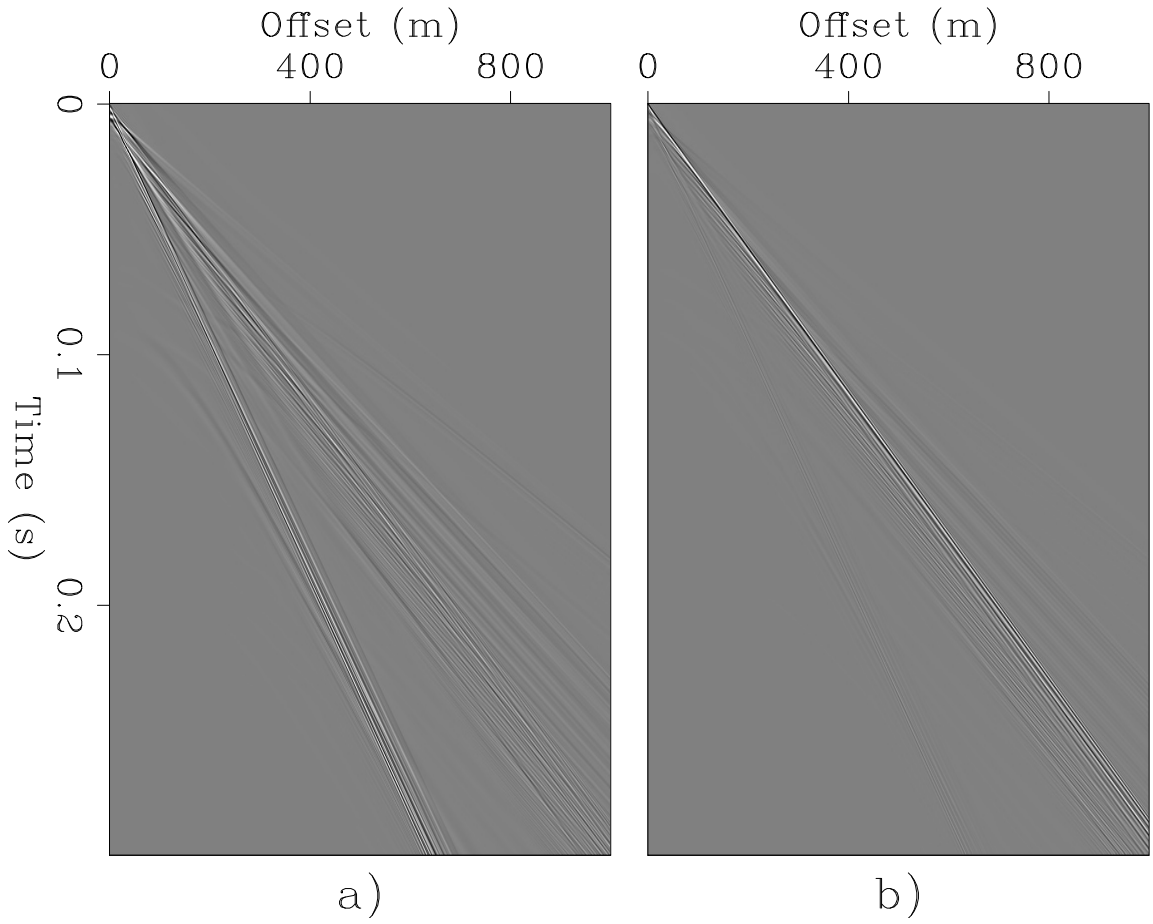

Figure 3: Comparison between data recorded by using a monopole (a) and a dipole (b) source. We display particle velocity along the horizontal direction. A dipole source excites mostly P-waves whereas a monopole one induces both P- and S- waves. [**CR**]

Figure 4: Relative amplitudes of P and S waves in a cross well acquisition setup. The distance between the wells is 260 m. Relative amplitudes are displayed as a function of horizontal distance between receiver and source. [**ER**]

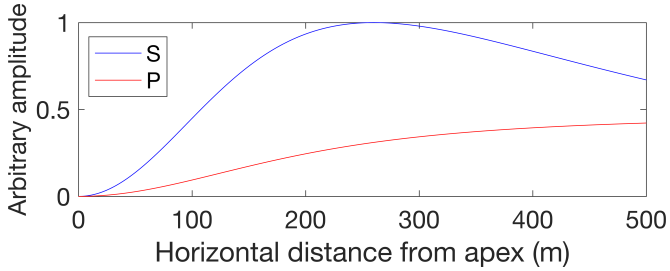

DATA SENSITIVITY TO THIN LAYERING

One of the potential applications of EFWI performed on single-well data is high-resolution imaging of thin layering within the reservoir. Given the high-frequency and dense receiver sampling of the DAS data, the layering within the reservoir could be imaged at much higher resolution than would be possible using any other type of seismic data. Furthermore, given the fairly dense shot sampling (approximately 10 meters) horizontal variations in reservoir layering may be also imaged. In particular, it would be useful to detect, and map along the well, high-velocity layers that might be related to volcanic intrusions that could act as a barrier to the fracturing induced by hydraulic stimulation. Such high-resolution imaging would be only possible if the existence of thin layers within the reservoir would have discernible effects on the recorded data. Therefore, we model data in three slightly different horizontally-layered models using the dipole source described in the previous section. The first is the simple three-layer model shown in Figure 5. The second includes a one-meter thick high-velocity layer (Figure 6); in the third model the high-velocity layer has the same elastic parameters as in Figure 6, but is two-meter thick.

Computed data for the two scenarios are shown in Figure 7. There are differences between recorded wavefields, indicating the sensitivity of the guided waves to thin layering. The more obvious changes are in the coda of the main arrival, which might be difficult to invert in presence of noise in the data. However, there are discernible changes in the phase of the main arrivals as well. No surprisingly, these changes are visible even at shorter offsets (200 meters) when comparing the data without and with the thick (2 meters) inclusion than when comparing the data without and with the thin (1 meter) inclusion. However, even in this less-favorable second case phase differences start to be visible at longer ($\geq$400 meters) offsets.

CONVERGENCE OF EFWI

Full-waveform inversion notoriously suffers from poor convergence when the starting velocity model is not sufficiently close to the true model and the recorded data miss low frequencies. The DAS field data presented in Lellouch et al. (2019b) are wideband but miss signal below 50 Hz. On the other hand, fairly high-quality data are available at short offset ($\geq$50 meters). At these offsets, the guided-waves effective propagation distance is similar to the recording offset and it is short. Therefore, the starting model needs to be significantly off for the recorded data and the data modeled with the starting model to be sufficiently out of phase to cause convergence problems.

For the application of imaging thin layering within the reservoir from single-well recordings that we have discussed in this paper a realistic assumption is that the starting model (Figure 5) is the average of the "true" model (Figure 2). More precisely, the velocities in the low-velocity zone (between depths of 93 and 108 meters) in Figure 5 are the reciprocal of the depth averages between 93 and 103 meters of the slownesses computed from the velocities shown in Figure 2. Figure 8 compares the

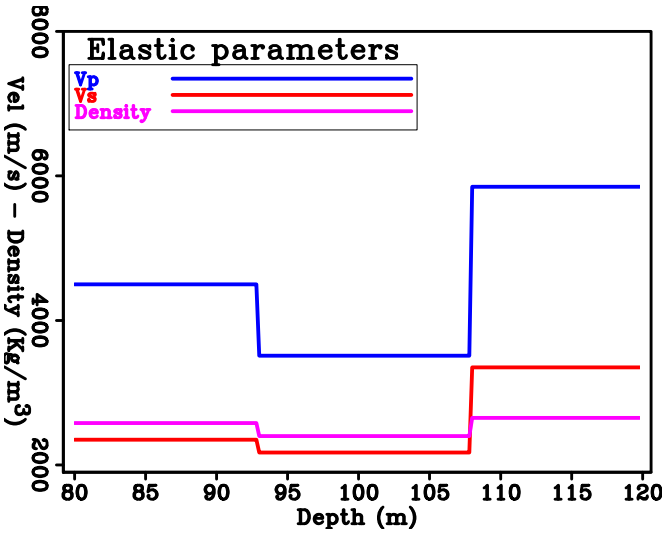

Figure 5: Elastic parameters for a simple 3-layers model. Source and receivers were placed at a depth of 100 m. [**ER**]

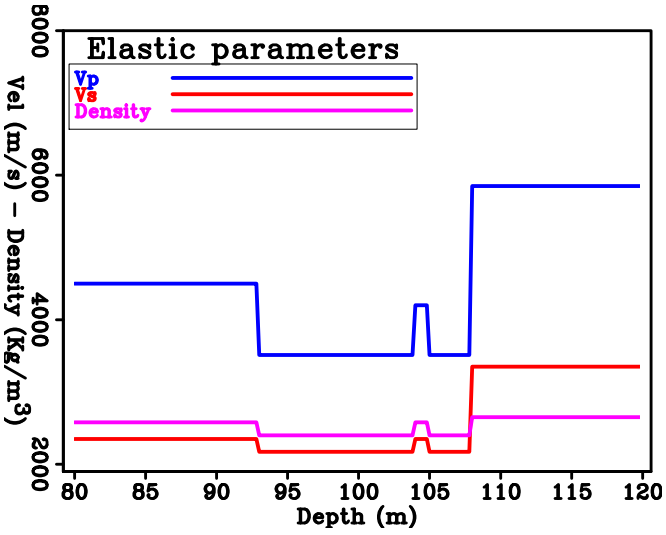

Figure 6: Elastic parameters for a simple 3-layers model (Figure 5) with an added one-meter thick intrusion. Source and receivers were placed at a depth of 100 m. [**ER**]

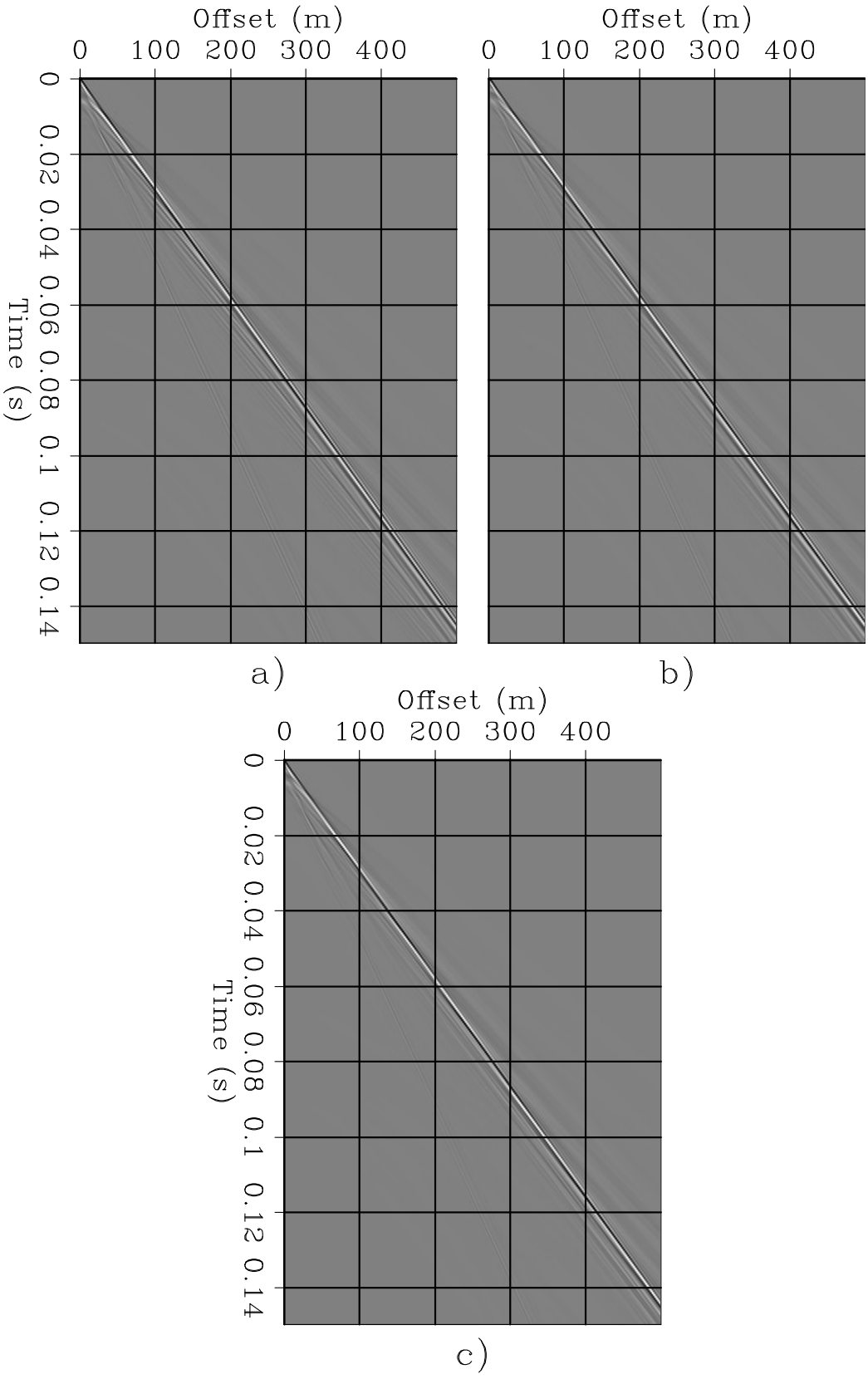

Figure 7: Data modeled using: a) a three-layer medium (Figure 5), b) a three-layer medium with a one-meter thick high-velocity inclusion (Figure 6), and c) a three-layer medium with a two-meter thick high-velocity layer. [**CR**]

full-bandwidth data (up to 900 Hz) modeled assuming the initial blocky model shown in Figure 5 (panel a) with the initial data residuals of a hypothetical EFWI process (panel b). We define the residuals as the differences between the data modeled using the "true" model (Figure 2) and the data modeled using the starting model. At full bandwidth and large offsets the two datasets have sufficiently phase differences that would cause "cycle-skipping" problems if we backprojected the data residuals to compute a search direction. However, when we zoom in into the near offsets (0-150 meters), as shown in Figure 9, we can observe that whereas there are visible phase differences between the two datasests, the gradient resulting from back-projecting the data residuals (panel b) is likely to produce useful search directions. Figure 10 compares the low frequencies of the two datasets shown in Figure 8 after applying a low-pass filter with corner frequency at 80 Hz. At large offsets, the phase differences between the two panels are clearly visible but still within a range that indicates useful search directions should be produced by back-projecting the residuals shown on the left panel of this figure. A more definitive answer to the convergence question can only be given when we will compute actual gradients and perform a full inversion; a task that we have not performed yet.

CONCLUSIONS AND FUTURE WORK

Thanks to their high frequency content and their sampling of the whole reservoir interval, guided waves are sensitive to high-resolution details of subsurface properties. Furthermore, cross-well recording may provide useful information on reservoir changes related to hydraulic stimulation and production.

This synthetic study sets the stage for the application of an elastic FWI (EFWI) workflow to guided waves. We show the recorded data is sensitive to thin layering (order of one meter) in the reservoir. We also show a multiscale FWI process that starts by inverting low frequencies and short offsets is likely to converge without encountering cycle-skipping problems. We assume that the starting model is based on approximate knowledge of reservoir elastic properties, as we may expect from geologic information and downhole logging or even by simple kinematic inversion of the same guided waves. We have not tested a full EFWI workflow on neither the synthetic data nor field data. The obvious next step will be to test such a workflow on synthetic data, and if successful, test it on field data.

This study is based on synthetic data and focuses on resolution and convergence. Elastic FWI applied to field data would encounter many additional practical challenges, such as: accuracy of the actual source locations, estimation of the time wavelet, and contamination of the recorded data by noise and inelastic effects.

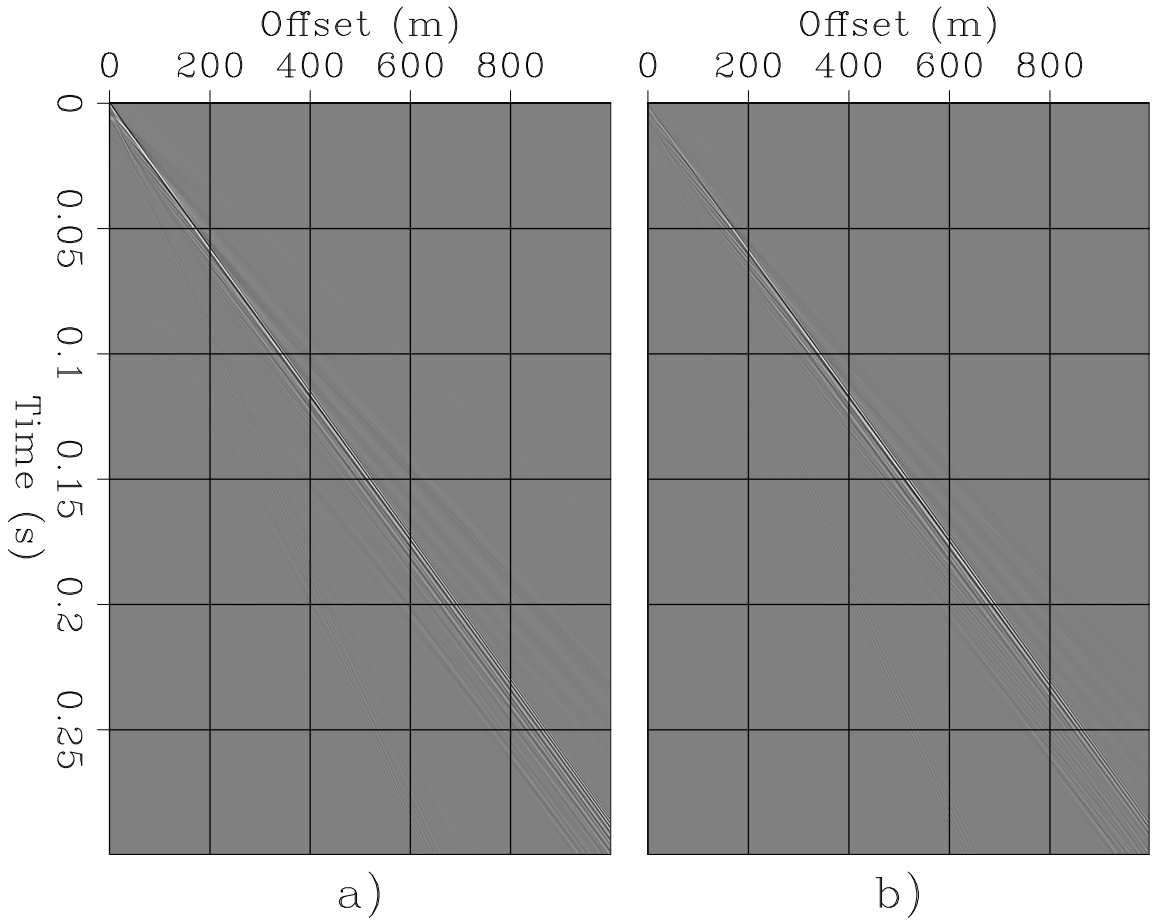

Figure 8: (a) Computed data assuming the three-layer model shown in Figure 5, and (b) the first data residuals when the "true" model is the realistic model shown in Figure 2. [**CR**]

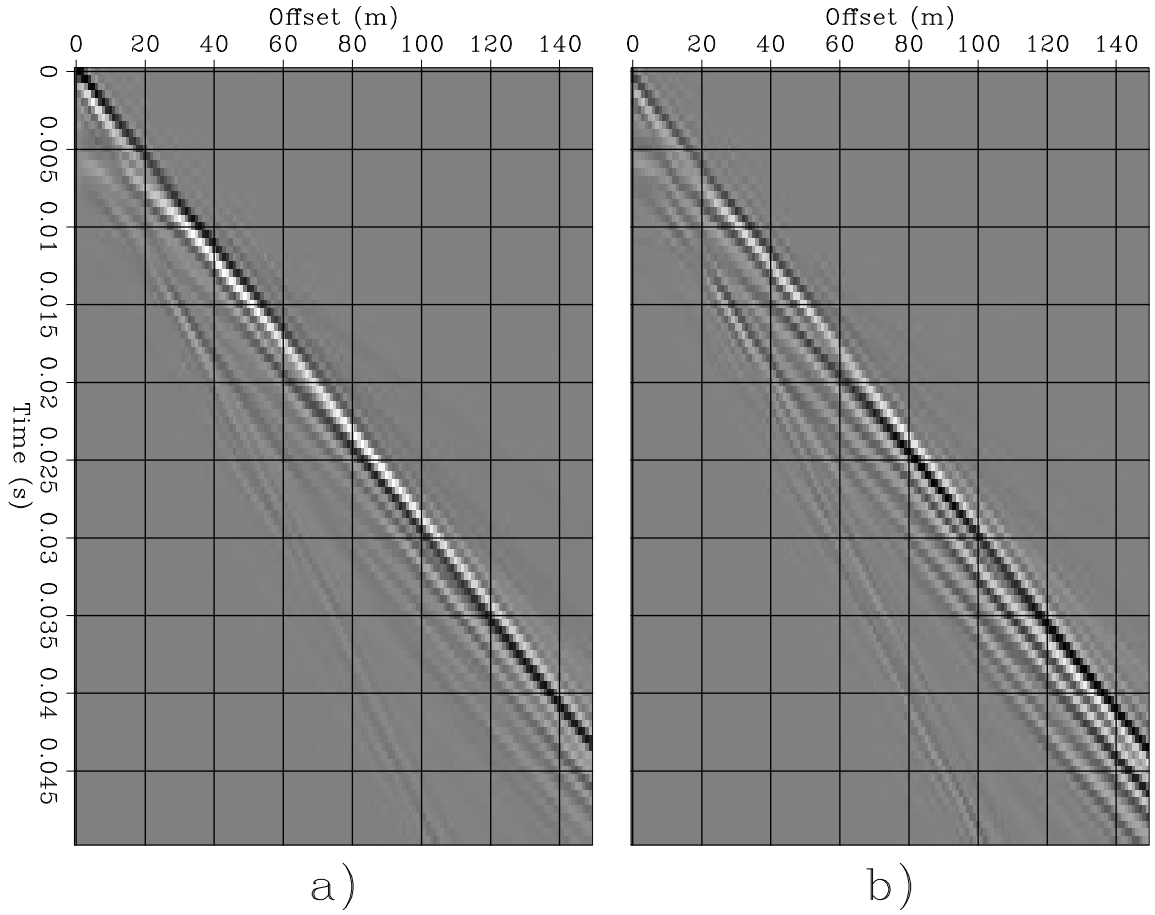

Figure 9: (a) Near 150 meters offsets of the computed data assuming the three-layer model shown in Figure 5, and (b) near 150 meters offsets of the first data residuals when the "true" model is the realistic model shown in Figure 2. [**CR**]

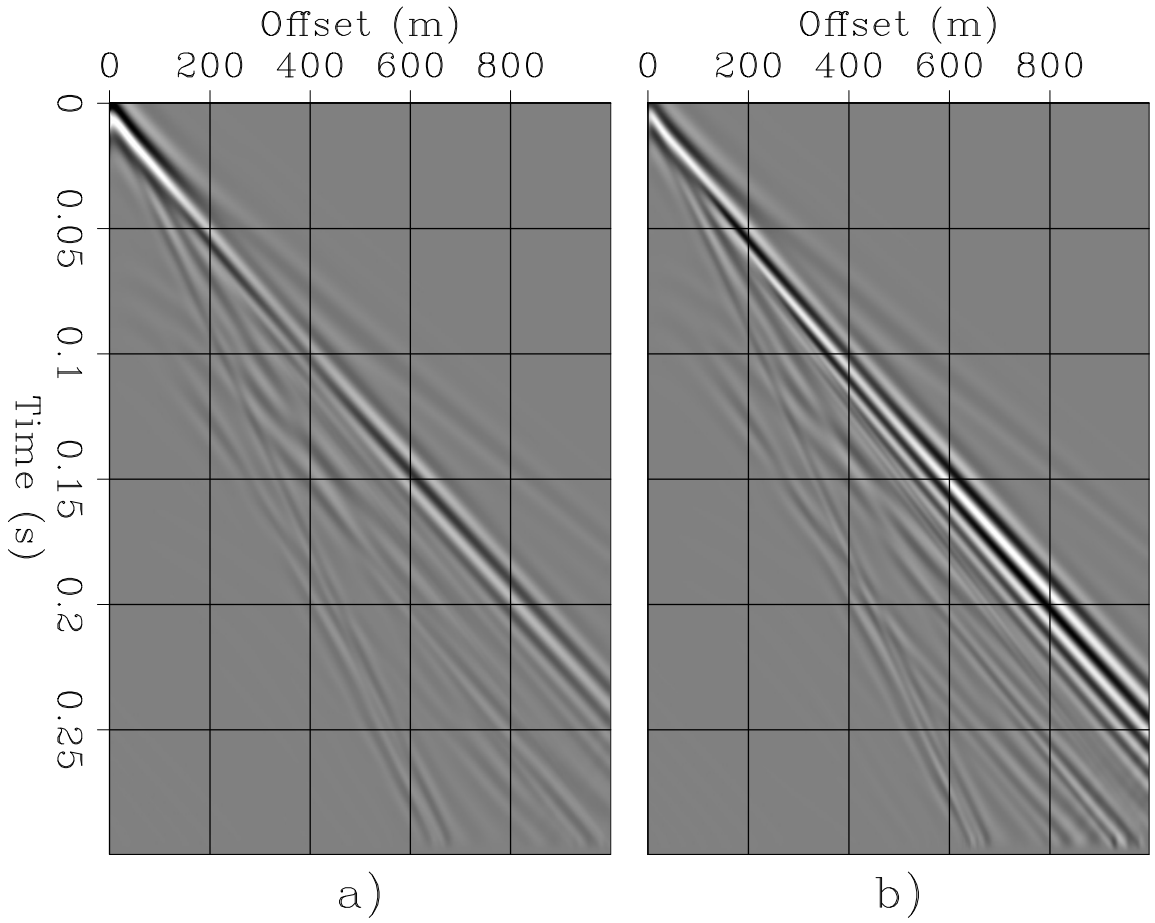

Figure 10: (a) Low frequencies (≤80 Hz) of the computed data assuming the three-layer model shown in Figure 5, and (b) low frequencies (≤80 Hz) of the first data residuals when the "true" model is the realistic model shown in Figure 2. [**CR**]

ACKNOWLEDGEMENTS

We would like to thank Mark Meadows for many interesting discussions, and Dimitri Bevc for (indirectly) pointing out to the paper by Fehler and Pearson we used to model the perforation shots as dipole sources.

REFERENCES

Fehler, M. and C. Pearson, 1984, Crosshole seismic surveys: Applications for studying subsurface fracture systems at a hot dry rock geothermal site: Geophysics, **49**, 37–45.

Lellouch, A., B. Biondi, S. Horne, M. A. Meadows, and T. Nemeth, 2019a, DAS observation of guided waves in a shale reservoir generated by perforation shots: SEG Technical Program Expanded Abstracts 2019, 943–947.

———, 2019b, DAS recordings of guided waves generated by perforation shots and propagating in a shale reservoir: SEP-Report, **176**, 101–110.

Lellouch, A., S. Horne, M. Meadows, S. Farris, T. Nemeth, and B. Biondi, 2019c, Das observations of perforation-induced guided waves in a shale reservoir: SEP-Report, **177**, EEE–FFF.

Martin, E. R., 2018, Passive Imaging and Characterization of the Subsurface With Distributed Acoustic Sensing: PhD thesis, Stanford University.